processes

MDPI

Article

Stability and Performance Analysis of Bioethanol Production with Delay and Growth Inhibition in a Continuous Bioreactor with Recycle

Rubayyi T. Alqahtani [1], Samir Kumar Bhowmik [2], Abdelhamid Ajbar [3,*] and Mourad Boumaza [3]

[1] Department of Mathematics and Statistics, College of Science, Imam Mohammad Ibn Saud Islamic University (IMSIU), Riyadh 11432, Saudi Arabia; rtalqahtani@imamu.edu.sa
[2] Department of Mathematics, University of Dhaka, Dhaka 1000, Bangladesh; bhowmiksk@gmail.com or bhowmiksk@du.ac.bd
[3] Department of Chemical Engineering, College of Engineering, King Saud University, Riyadh 11432, Saudi Arabia; mouradb@ksu.edu.sa
* Correspondence: aajbar@ksu.edu.sa

Abstract: This paper proposes and analyzes a mathematical model for the production of bioethanol in a continuous bioreactor with recycling. The kinetics correspond to the use of *Saccharomyces bayanus* for the fermentation of sugars found in wastewater from soft drinks. The proposed model considers product growth latency, which was experimentally found in batch studies of ethanol production. Furthermore, the inhibition effect of ethanol is expressed by a modified version of the classical Andrew's model for substrate inhibition. The proposed model consists of only three ordinary differential equations containing a minimal number of operating parameters, which include the bioreactor residence time, glucose feed concentration, recycle ratio and the fraction of biomass removed from the reactor by the flow. The positivity and the boundedness of solutions of the model were confirmed under reasonable restrictions of parameters. The stability analysis showed that there is a value of residence time at which an exchange of stability occurs between the trivial washout and non-washout solutions. This critical value depends only on the substrate feed concentration, biomass death rate, recycle ratio and purge fraction. Dynamic simulations of the model were carried out for substrate concentration in the range of 100–250 g/L, commonly used for the production of ethanol. An inverse response due to the inhibition effects of ethanol was observed in the time evolution of substrate and biomass concentrations. Parametric studies showed that ethanol concentration increases with the recycle ratio, with the inverse of residence time and with the inverse of purge fraction. The effect of ethanol latency has, on the other hand, a substantial effect on ethanol concentration. Despite its unstructured nature and the fact that some parameters such as temperature and acidity were not taken into consideration, the proposed model managed to provide useful results on the bioreactor-settler stability and the effect of key parameters on its dynamic behavior, which could pave the way for future optimization studies.

Keywords: bioreactor; continuous; model; delay; *Saccharomyces bayanus*; ethanol; stability; performance

Citation: Alqahtani, R.T.; Bhowmik, S.K.; Ajbar, A.; Boumaza, M. Stability and Performance Analysis of Bioethanol Production with Delay and Growth Inhibition in a Continuous Bioreactor with Recycle. *Processes* **2021**, *9*, 461. https://doi.org/10.3390/pr9030461

Academic Editor: Antonio D. Moreno

Received: 8 February 2021
Accepted: 24 February 2021
Published: 4 March 2021

1. Introduction

The growing demand for petrifaction and fossil fuels due to the swift revolution of automotive industries and modern societies has been inspired the study of developing alternative fuels for combustion engines for decades. Environmental pollution issues are also pushing scientists and industrialists to search for alternatives to fossil fuels [1]. Sincere attention has been given to inventing/discovering a sustainable, clean and cheap alternative to satisfy modern smart environmental needs [2,3].

Bioethanol is one of the best alternatives to oil-derived fossil fuels. Ethanol extracted from suitable renewable sources is carbon friendly and an attractive green energy to control environmental contamination and reduce dependence on petrifaction and fossilized carbon

energy [4,5]. Ethanol is also one of the most efficient and attractive substitutes for fuels, either when blended with gasoline or used as a fuel-ethanol. More recently, it has received attention for its use as an oxygenate for the control of automotive tailpipe emissions. Alcohols are also used successfully as substitutes of gasoline ether oxygenates [6].

Nowadays, a variety of agricultural products, such as sorghum, corn, sugar cane, wheat, carrot and cassava [7–10], are used as main substrates for bioethanol production. In this aspect, one important type of work reported in the literature is to extract the kinetics of batch fermentation using the aforementioned raw materials. This task involves the selection of suitable yeast strains, the extraction of the kinetic model and the determination of media's optimal operating conditions. However, another important challenge consists of the design of large-scale ethanol continuous processes. This is an area where relatively less work has been carried out compared to batch processes [11–13]. This field is also quite challenging since it is known that the process of bioethanol production by continuous fermentation is highly complex and nonlinear [14]. The nonlinearity manifests itself in the occurrence of phenomena such as bistability [15] and stable limit cycles [11].

The development of mathematical models for continuous ethanol processes can be a very useful tool, which can be applied to explore the complex phenomena that occur in industrial ethanol continuous processes [11–16]. On another, equally important level, these mathematical models can also be used for parametric studies and to offer insight into ways to increase the productivity of the process.

The main purpose of this study is to propose a rigorous yet reasonably simple model for ethanol production in a well-stirred continuous bioreactor with recycling. The model will be used to analytically investigate the stability of the reactor–settler system and to carry out numerical simulations to investigate the effects of the different system parameters on ethanol concentration. In order to make the analysis a realistic one, the kinetic parameters were extracted from batch studies carried out in [2,3] on the use of *Saccharomyces bayanus* for the fermentation of sugars contained in industrial wastewater from soft drinks. In order to describe the inhibition effect of ethanol on the growth rate, the authors tested a number of growth rate expressions and found that an expression similar to Andrew's expression [17], commonly used to describe substrate inhibition, was most suitable for fitting their experimental data. The authors developed a mathematical model for the batch process that satisfactorily described sugar consumption, biomass growth, and bioethanol production. The researchers in [3] also observed a latency of ethanol production in their experiments.

Besides incorporating the kinetics associated with decay, maintenance and growth delay based on the aforementioned work of [3], the proposed model in this study incorporates key operating parameters that can influence the performance of the bioreactor, namely the residence time, the recycle ratio and the purge fraction.

The rest of the article is organised as follows. In Section 2, we propose our nonlinear model with a delay. A set of important properties of the model is discussed in Section 3. The steady states and the stability properties of such steady states are studied in Sections 4 and 5. A numerical illustration and conclusion are drawn in Section 6.

2. Mathematical Model

In this section, we present the model equations that describe the dynamics of a well-stirred continuous bioreactor with cell recycling shown schematically in the diagram of Figure 1. The mass balances of substrate (S), biomass (X) and ethanol (E) yield the following ordinary differential equations

$$V\frac{\mathrm{d}S}{\mathrm{d}t} = F(S_0 - S) - \frac{\mu_{\max}}{Y_{x/s}} \cdot M(S,E) \cdot X \cdot V, \tag{1}$$

$$V\frac{\mathrm{d}X}{\mathrm{d}t} = -F\beta_1 X + \mu_{\max} \cdot M(S,E) \cdot X \cdot V + RF(C-1)X - b_H VX, \tag{2}$$

$$V\frac{\mathrm{d}E}{\mathrm{d}t} = -F\beta_2 E + Y_{e/x}\, \mu_{\max} \cdot M(S,E) e^{-(pS)^q} \cdot X \cdot V + V\gamma X, \tag{3}$$

V is the rector volume, F the volumetric flow rate, S_f the concentration of the substrate feed, μ_{max} the maximum specific growth rate, $Y_{x/s}$ the biomass yield coefficient, $Y_{e/x}$ the ethanol/biomass yield coefficient, b_H the biomass death rate coefficient and γ is the kinetic constant of ethanol production by maintenance. The specific growth rate is denoted by $M(S, E)$ and is a function of both substrate and ethanol concentrations, since it is known that the growth rate is inhibited by ethanol concentration [2,3]. A number of growth rate models were proposed in the literature, but here, we adopt the following expression proposed by [3]

$$M(S, E) = \frac{S}{K_s + S + K_e E^2}, \tag{4}$$

where K_s is the saturation constant and K_e the inhibition constant by ethanol. The form of Equation (4) is inspired by the expression used in the case of pure substrate inhibition $\frac{S}{K_s+S+K_eS^2}$, which is known as Andrew's growth model [17]. As was mentioned in the introduction, the choice of the expression in Equation (4) was guided by the experimental work carried out in [3] on the growth of *Saccharomyces bayanus* on wastewater from soft drinks. Moreover, to account for latency in ethanol production, a term dependent only on sugar concentration [3] was included in the ethanol mass balance (Equation (3)). The reactor residence time is defined by

$$\tau = \frac{V}{F} \tag{5}$$

In Equation (2), the term CX represents the biomass concentration in the flow leaving the separating unit. The value of the concentrating factor (C) depends upon the design and operation of the settling unit. It is also highly dependent on recycle properties such as settling, and compressibility behavior. The term β_1, on the other hand, represents the fraction of the biomass that leaves the reactor (purge fraction). A mass balance around the settling unit shows that the maximum value of the concentrating factor is given by

$$C_{max} = 1 + \frac{1}{R} \tag{6}$$

Thus, the maximum value of the product $R(C-1)$ is

$$|R(C-1)|_{max} = 1 \tag{7}$$

The coefficient β_2 in Equation (3) represents, on the other hand, the fraction of ethanol in the feed. For practical reasons, this fraction is negligeable or nonexistent, and therefore a zero value is assumed for β_2. The model is supplemented with an initial profile satisfying

$$S(0) = S_0 \geq 0,\ X(0) \geq 0,\ E(0) \geq 0 \tag{8}$$

It can be seen that, for particular laboratory environmental conditions, the kinetic parameters K_e, K_s, $Y_{x/s}$, $Y_{e/x}$, b_H, γ, p,q and $\mu_{\max}$ are all fixed. The operating parameters that one may vary are S_0, R, β_1 and τ.

The values of the kinetic parameters are shown in Table 1.

Table 1. Dimensional parameters values.

Parameters	Values	Unit	Reference
$\mu_{\max}$	0.606	h^{-1}	[3]
b_H	0.00916	h^{-1}	[18]
p	1.188×10^{-6}	$g_{ethanol}/g_{biomass}$	[3]
q	3.038	g / L	[3]
S_0	100	g / L	[3]
$Y_{x/s}$	0.066	$g_{biomass}/g_{substrate}$	[3]
$Y_{e/x}$	9.227	$g_{ethanol}/g_{biomass}$	[3]
K_e	0.029	$L\, g_{substrate}/g^2_{ethanal}$	[3]
K_s	65.535	$g_{substrate}/L$	[3]
γ	0.001	$g_{ethanol}/g_{biomass}/h$	[3]

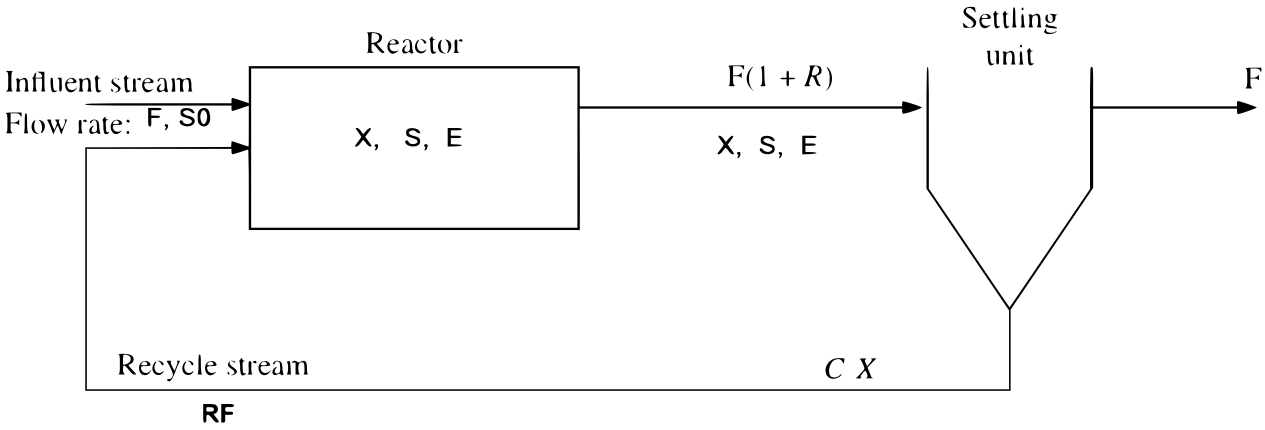

Figure 1. Schematic diagram of the bioreactor-settler system.

The Dimensionless Model

The model is rendered dimensionless using the following variables: $[S^* = S/K_s]$, $[X^* = X/Y_{x/s}K_s]$, $[E^* = E/K_s]$ and $[t^* = \mu_{\max}t]$. The system of ODE (1)–(3) can be written in a dimensionless form by

$$\frac{dS^*}{dt^*} = \frac{S_0^* - S^*}{\tau^*} - \frac{X^*S^*}{1 + S^* + \gamma_1 E^{*^2}}, \tag{9}$$

$$\frac{dX^*}{dt^*} = \frac{-\beta_1 X^*}{\tau^*} + \frac{X^*S^*}{1 + S^* + \gamma_1 E^{*^2}} - b_H^* X^* + \frac{R_1^* X^*}{\tau^*}, \tag{10}$$

$$\frac{dE^*}{dt^*} = \frac{-\beta_2 E^*}{\tau^*} + \gamma_2 X^* + \gamma_3 \left[\frac{X^*S^*}{1 + S^* + \gamma_1 E^{*^2}}\right] e^{-(p^*S^*)^q}. \tag{11}$$

All the dimensionless parameters here are non-negative. A short tabular description of the model parameters is given in Nomenclature section. Looking at the dimensionless parameter $R^* = R(C - 1)$ that represents the effective recycle ratio, it can be seen that the maximum value of R^* is 1. On the other hand, the choice of $\beta_1 = 1$ gives a continuous flow reactor with recycle. Therefore, the cases $R^* = 1$ and $0 < R^* < 1$ with $\beta_1 = 1$ define a flow reactor with ideal and non-ideal recycle respectively. The values of the model dimensionless parameters (computed using the dimensional values of Table 1) are given in Table 2. Besides the fixed kinetic parameters, the nominal values of operating parameters are also shown in the table. Specifically, the glucose feed concentration S_0 has a nominal value of 100 g/L, which corresponds to $S_0^* = 1.53$. It should be noted that the range of sugar concentrations commonly used for the production of ethanol is about 100–250 g/L.

Table 2. Dimensionless parameters values.

Parameters	Values
β_1	1
β_2	0
γ_1	1.9
γ_2	6.6×10^{-5}
γ_3	0.609
τ^*	12
b_H^*	0.0151
p^*	7.786×10^{-5}
R^*	1.0

3. Mathematical Analysis

Uniqueness, uniform boundedness and invariance of solutions play an important role in mathematical modeling, since these stated properties reflect the physically meaningful features of the problem. To that end, we begin here by studying the uniqueness properties of solutions followed by the boundedness and invariance of model solutions over the following physically meaningful domain

$$\Omega = \Big\{(Z_1, Z_2, Z_3) \in \mathbb{R}^3 | Z_1 \geq 0, Z_2 \geq 0, Z_3 \geq 0\Big\}, \quad \text{and} \quad J = [0, T], T >> 0.$$

To facilitate our study a variable $Z \in \mathbb{R}^3$ is defined by

$$Z = (Z_1, Z_2, Z_3) := (S^*, X^*, E^*).$$

Using the new set of redefined variables, the model (9)–(11) is written as

$$\frac{d}{dt}Z = F(Z), \quad \text{with a given initial condition } Z(0) = Z_0 \geq 0, \tag{12}$$

where $F : \mathbb{R}^3 \to \mathbb{R}^3$, and $F_i : \mathbb{R}^3 \to \mathbb{R}$, $i = 1,\ 2,\ 3$ are given by

$$F(Z) = [F_1(Z), F_2(Z), F_3(Z)],$$

with

$$\begin{aligned} F_1(Z) =& \frac{S_0^* - Z_1}{\tau^*} - \mathcal{M}(Z)Z_2, \\ F_2(Z) =& \frac{-\beta_1 Z_2}{\tau^*} + \mathcal{M}(Z)Z_2 - b_H^* Z_2 + \frac{R^* Z_2}{\tau^*}, \\ F_3(Z) =& \frac{-\beta_2 Z_3}{\tau^*} + \gamma_2 Z_2 + \gamma_3 \mathcal{M}(Z) Z_2 e^{-(p^* Z_2)^q}. \end{aligned}$$

Here, the modified function

$$\mathcal{M} : \mathbb{R}^3 \to \mathbb{R}$$

is given by

$$\mathcal{M}(Z) = \frac{Z_1}{1 + Z_1 + \gamma_1 Z_3^2}. \tag{13}$$

It is obvious that $0 \leq \mathcal{M}(Z) \leq 1$, $\forall\ Z \in \Omega$. The time evolution of the growth rate of biomass (Z_1), consumption of substrate (Z_2), and ethanol production (Z_3) are described by (12). Now, it is our aim to investigate if the solutions of (12) are positive. This step is necessary to see if the model is physically meaningful. To facilitate the analysis, we enforce a few physically reasonable restrictions

H_1 : Parameters used here belong to $\mathbb{R}_+$.

H_2 : $\beta_1 + \tau^* b_H^* \leq R^* + \tau$.

H_3 : $\beta_2 \leq (\gamma_2 + \gamma_3)\tau$.

H_4 : $0 \leq R^* < 1$.

The assumptions H_1, H_2, H_3 and H_4 represent physically meaningful restrictions on the model parameters.

Theorem 1. *Assume that H_1–H_4 hold, then there exists a bounded unique solution to the initial value problem (12) over J.*

Proof. Here, the gradient of $F(Z)$ exists for all $Z \in \Omega$. We can see that $|\mathcal{M}(Z)| < 1$ for all $Z \in \Omega$. Applying H_1–H_4 leads to

$$|F_1(Z)| \leq \frac{S_0^*}{\tau^*} + \frac{1}{\tau^*}\|Z\|,$$

$$|F_2(Z)| < \left(1 + \frac{R^* - B_H^*\tau - \beta_1}{\tau^*}\right)\|Z\|$$

and

$$|F_3(Z)| < \left(-\frac{\beta_2}{\tau^*} + \gamma_2 + \gamma_3\right)\|Z\|.$$

Thus,

$$\|F\|_\infty < C_1\|Z\| + C_2,$$

where

$$C_1 = \max\left\{\frac{1}{\tau^*}, \left(1 + \frac{R^* - B_H^*\tau - \beta_1}{\tau^*}\right), \left(-\frac{\beta_2}{\tau^*} + \gamma_2 + \gamma_3\right)\right\}$$

and

$$C_2 = \frac{S_0^*}{\tau^*}.$$

Thus, Equation (12) has a unique solution which is also bounded [19,20]. □

Theorem 2. *Assume that along with H_1,*

H_5 : $\beta_1 + b_H\tau \geq R + \tau(\gamma_2 + \alpha\gamma_3)$ *for some* $0 < \alpha << 1$.

holds. Then, the integral $Z(t)$ of (12) is a uniformly bounded solution over $\bar{\Omega}$ if $z_0 \in \Omega$ satisfies $|z_0| < \infty$.

Proof. Let us define

$$U = Z_1 + Z_2 + Z_3.$$

Then, using the fact that

$$\mathcal{M}(Z)e^{-(p^*Z_1)^q} \leq 1, \ \forall \ Z \in \Omega$$

we obtain

$$\frac{dU}{dt} = -C_1U + C_2,$$

where

$$0 < C_1 \leq \min\{A, B, C\}$$

with

$$A = \frac{1}{\tau}, \ B = \frac{\beta_1}{\tau} + b_H - \frac{R}{\tau} - \gamma_2 - \alpha\gamma_3, \ C = \frac{\beta_2}{\tau} \text{ and } \ C_2 = \frac{S_0^*}{\tau},$$

where $\alpha = |\mathcal{M}(Z)e^{-(p^*Z_2)^q}| << 1$ which completes the proof. □

Now, we focus on showing the invariance of integral $Z(t)$ of (12) in Ω.

Theorem 3. *Ω is a positively invariant set for the integral Z if H_1 holds.*

Proof. Consider the domains

Set 1 : $Z_1 = 0$, $Z_2 > 0$, and $Z_3 \geq 0$,
Set 2 : $Z_2 = 0$, $Z_1 \geq 0$, and $Z_3 > 0$,
Set 3 : $Z_3 = 0$, $Z_1 > 0$, and $Z_2 \geq 0$,
Set 4 : $Z_1 \geq 0$, $Z_2 = 0$, and $Z_3 = 0$,

on the boundary and the edges of Ω. Then

$$\frac{dZ_1}{dt} = \frac{S_0^*}{\tau^*} > 0,$$

for the **Set 1**. Thus, Z_1 is inside Ω. For **Set 2**, we have

$$\frac{dZ_2}{dt} = 0,$$

and this guarantees that Z_2 resides inside the domain Ω. Now, for **Set 3**, we have

$$\frac{dZ_3}{dt} = \gamma_2 Z_2 + \gamma_3 \mathcal{M}(Z) Z_2 e^{-(p^* Z_2)^q},$$

which also shows that $Z_3 \in \Omega$. We can show that

$$\frac{dZ_1}{dt} = \frac{S_0^* - Z_1}{\tau^*}, \ \frac{dZ_2}{dt} = 0, \ \frac{dZ_3}{dt} = 0$$

for **Set 4**. Thus, all the cases confirm that $Z \in \Omega$. Hence, the solution domain Ω is invariant [21]. □

Now, we analyze the parameter dependence of the solution trajectories of the dimensionless model (9)–(11). Let

S 1 : $\{S_0^{*,1}, \tau^{*,1}, p^{*,1}, q^1, \beta_1^{*,1}, \beta_2^{*,1}, \gamma_1^1, \gamma_2^1, \gamma_3^1, R^{*,1}\}$ be the parameter Set 1 for (9)–(11) with integrals $Y(t) \in \mathbb{R}^3_+$.

S 2 : $\{S_0^{*,2}, \tau^{*,2}, p^{*,2}, q^2, \beta_1^{*,2}, \beta_2^{*,2}, \gamma_1^2, \gamma_2^2, \gamma_3^2, R^{*,2}\}$ be the parameter Set 2 for (9)–(11) with integrals $Z(t) \in \mathbb{R}^3_+$.

Now, let recall that

$$\left| \frac{1}{1 + Y_1 + \gamma_1 Y_3^2} \right| \leq 1 \text{ and } 0 \leq \mathcal{M}(Y) \leq 1, \text{ if } Y = [y_1, y_2, y_3]' \in \mathbb{R}^3_+.$$

We need the following lemma to analyze parameter estimation.

Lemma 1. *Let $Z(t)$ be the trajectory of the model with initial value Z_0, and γ, $C \geq 0$ be the constants such that the following linear growth condition holds [22]*

$$\|\dot{Z}(t)\| \leq \gamma \|Z(t)\| + C, \ \forall \ t \geq 0,$$

then the inequality

$$\|Z(t) - Z_0\| \leq \|Z_0\|(e^{\gamma t} - 1) + \frac{C}{\gamma} e^{\gamma t}, \ \forall \ t \geq 0, \text{ holds.}$$

Theorem 4. *Let $Y(t)$ and $Z(t)$ be two integrals of the system of differential Equations (9)–(11) with parameter sets S1 and S2, $R^* \geq B_2^*$ and initial profiles Y_0 and Z_0, respectively; then*

$$\|Y - Z\| \leq \|Y_0 - Z_0\| e^{C^* t} + C_1 e^{C^* t},\ t \geq 0,$$

holds where $C^* \geq 0$ and $C_1 \geq 0$ are constants.

Proof. Let $Y(t)$ and $Z(t)$ be two integrals for the system (9)–(11), then

$$\|\dot{Y} - \dot{Z}\| = \|f(Y) - f(Z)\| = \sum_{i=1}^{3} |f_i(Y) - f_i(Z)|.$$

Now

$$|F_1(Y) - F_1(Z)| = \left| \frac{S_0^{*,1} - Y_1}{\tau^{*,1}} - \frac{S_0^{*,2} - Z_1}{\tau^{*,2}} \right| + |\mathcal{M}(Y)Y_2 - \mathcal{M}(Z)Z_2|$$

and thus

$$|F_1(Y) - F_1(Z)| \leq C_1 + C_2\|Y - Z\|$$

where C_1 and C_2 depend on the parameters. Similarly, using the fact that $0 \leq \mathcal{M}(Z) \leq 1$ for all $Z \in \Omega$ yields

$$|F_2(Y) - F_2(Z)| \leq C_3\|Y - Z\|$$

where C_3 depends on the parameters. Additionally,

$$\begin{aligned} |F_3(Y) - F_3(Z)| &\leq \left| \left(-\frac{\beta_2^1}{\tau^{*,1}} + \frac{R^{*,1}}{\tau^{*,1}} \right) Y_3 - \left(-\frac{\beta_2^2}{\tau^{*,2}} \right) Z_3 \right| \\ &\quad + \left| (\gamma_2^1 + \gamma_3^1)Y_2 - (\gamma_2^1 + \gamma_3^1)Z_2 \right| \\ &\leq C_4|Y_2 - Z_2| + C_5|Y_3 - Z_3| \leq C_6\|Y - Z\| \end{aligned}$$

where $C_6 = \max\{C_4, C_5\}$,

$$C_4 = \max\left\{ -\frac{\beta_2^1}{\tau^{*,1}} + \frac{R^{*,1}}{\tau^{*,1}}, -\frac{\beta_2^2}{\tau^{*,2}} \right\},$$

and

$$C_5 = \max\left\{ \gamma_2^1 + \gamma_3^1, \gamma_2^1 + \gamma_3^1 \right\}$$

since

$$0 \leq \mathcal{M}(Z)e^{-(p^* S^*)^q} \leq 1 \text{ for all } Z \in \Omega.$$

A combination of all the above inequalities yields

$$\|\dot{Y} - \dot{Z}\| \leq C_1 + C^*\|Y - Z\|$$

where $C^* = \max\{C_2, C_3, C_6\}$. Thus applying Lemma 1 yields

$$\|Y - Z\| \leq \|Y_0 - Z_0\| e^{C^* t} + C_1 e^{C^* t},\ t \geq 0,$$

which completes the proof. □

4. Equilibria

The objective in this section is to find steady-state solutions of the nonlinear system

$$F(Z) = 0 \quad \text{where} \quad F(Z) = \begin{bmatrix} F_1(Z) \\ F_2(Z) \\ F_3(Z) \end{bmatrix},$$

with

$$\begin{aligned} F_1(Z) =& \frac{S_0^* - S^*}{\tau^*} - \mathcal{M}(Z)X^*, \\ F_2(Z) =& \left(\frac{-\beta_1}{\tau^*} + \mathcal{M}(Z) - b_H^* + \frac{R^*}{\tau^*} \right) X^*, \\ F_3(Z) =& \frac{-\beta_2 E^*}{\tau^*} + \gamma_2 X^* + \gamma_3 \mathcal{M}(Z) E^* e^{-(p^* S^*)^q}. \end{aligned}$$

It can be noted that $Z_0^* = (S_0^*, 0, 0)$ is always a washout solution of the nonlinear system $F(Z) = 0$ in Ω. This solution is not desirable since it indicates that no biological process has occurred. We now look for a non-trivial solution (non-washout) to the nonlinear system of equations $F(z) = 0$ in Ω, considering some physically meaningful restrictions on parameter values. Let

$$F_2(Z) = 0 \text{ gives } \mathcal{M}(Z) = a_1,$$

where

$$a_1 = (\beta_1 - R_1^*) + b_h^* \tau^* > 0. \tag{14}$$

Now, adding $F_1(Z) = 0$ and $F_2(Z) = 0$ yields

$$X^* = \frac{S_0 - S^*}{a_1 \tau^*}. \tag{15}$$

Substituting the value of X^* (Equation (15)) in $F_1(Z) = 0$ yields

$$E^* = \frac{\sqrt{a_1 \gamma_1 (S^*[1 - a_1] - a_1)}}{a_1 \gamma_1}. \tag{16}$$

From equation ($F_1(Z) = 0$), we have

$$\frac{X^* S^*}{1 + S^* + \gamma_1 E^{*^2}} = \frac{S_0 - S^*}{\tau^*}. \tag{17}$$

Thus, substituting Equation (15) in Equation (17) results in

$$E^{*^2} = \frac{(S^*[1 - a_1] - a_1)}{a_1 \gamma_1}. \tag{18}$$

Note that the right side of Equation (18) must be positive since the left side is E^{*2}. Thus, the expression inside the square root in Equation (16) is positive. Now, substituting Equations (15), (17) and (18) in $F_3(Z) = 0$ yields

$$b_1 \, y^2 + b_2 \, y + b_3 = 0, \tag{19}$$

where

$$\begin{aligned} y =& e^{-(p^* S^*)^q}, \quad b_1 = (a_1 \gamma_3 \tau^* (S^* - S_0^*))^2, \quad b_2 = 2 a_1 \gamma_2 \gamma_3 \tau^{*^2} (S^* - S_0^*)^2, \\ b_3 =& (\gamma_2 \tau (S^* - S_0^*))^2 - [\beta_2 \, a_1]^2 \left(\frac{1 + S^*}{{\gamma_1}^2} + \frac{S^* \, \tau^*}{a_1 \, \gamma_1} \right). \end{aligned}$$

5. Stability of the Equilibria

Stability analysis is at the heart of dynamical analysis. Only stable solutions can be noticed experimentally. Thus, it is very important to analyze the stability of an ODE system. Mostly researchers rely on the eigenvalues of the Jacobian matrix relevant to the nonlinear dynamical system. The Jacobian of the system of ODE (9)–(11) can be presented by

$$\mathrm{J}(S^*, X^*, E^*) = \begin{bmatrix} -[\frac{1}{\tau} + A_4] & -A_2 & A_3 \\ A_4 & A_5 & -A_3 \\ A_7 & A_8 & -A_9 \end{bmatrix},$$

where

$$A_1 = \frac{1}{\tau^*} + A_4 \quad A_2 = \frac{S^*}{1 + S^* + \gamma_1 E^{*^2}},$$

$$A_3 = \frac{2\gamma_1 X^* S^* e^*}{\left(1 + S^* + \gamma_1 E^{*^2}\right)^2}, \quad A_4 = \frac{X^*\left(1 + \gamma_1 E^{*^2}\right)}{\left(1 + S^* + \gamma_1 E^{*^2}\right)^{*^2}},$$

$$A_5 = \left[\frac{(R^* - \beta 1) - \tau^* b_H^*}{\tau^*}\right] + \frac{S^*}{1 + S^* + \gamma_1 E^{*^2}},$$

$$A_6 = -A_3, \quad A_7 = -\frac{q(p^* S^*)^q [e^{-(p^* S^*)^q}] fl_3\, X^*}{\left(1 + S^* + \gamma_1 E^{*^2}\right)} + \frac{[e^{-(p^* S^*)^q}] fl_3\, X^*\left(1 + \gamma_1 E^{*^2}\right)}{\left(1 + S^* + \gamma_1 e^{*^2}\right)^2},$$

$$A_8 = \gamma_2 + \frac{\gamma_3 S^* [e^{-(p^* S^*)^q}]}{1 + S^* + \gamma_1 e^{*^2}}, \quad A_9 = \frac{(\beta_2)}{\tau^*} + \frac{2\gamma_3 \gamma_1 X^* S^* e^* [e^{-(p^* S^*)^q}]}{\left(1 + S^* + \gamma_1 E^{*^2}\right)^2}.$$

The eigenvalues of $J(S^*, X^*, E^*)$ evaluated at the washout steady-state can be presented by

$$\begin{aligned} \lambda_1 &= -\frac{1}{\tau^*} < 0, \\ \lambda_2 &= -\left[\frac{\beta_2}{\tau^*}\right] < 0, \\ \lambda_3 &= \frac{R^* - \beta_1}{\tau^*} + \frac{S_0^* - b_H^*(1 + S_0^*)}{1 + S_0^*}. \end{aligned} \tag{20}$$

Therefore, it follows from the sign of eigenvalues that the washout branch is always stable if the following restriction holds

$$b_H^* \geq \frac{S_0^*}{1 + S_0^*}. \tag{21}$$

Performing similar results as shown in [23], we can see that the washout solution is globally stable when the following restriction of parameters holds $b_H^* \geq \frac{S_0^*}{1+S_0^*}$. If $b_H^* < \frac{S_0^*}{1+S_0^*}$ we conclude from Equation (20) that the washout steady-state is always stable provided that

$$\tau^* < \tau_{\mathrm{cr}}^* = \frac{(1 + S_0^*)(\beta_1 - R^*)}{S_0^* - b_H^*(1 + S_0^*)}. \tag{22}$$

It can be noted that the washout solution is never stable when $R^* = \beta_1$. Therefore, we end up with the following result.

Lemma 2. *The washout solutions $X_0^* = (S_0^*, 0, 0)$ are locally asymptotically stable provided the condition (22) is satisfied.*

The Jacobian matrix relevant to the non-washout solution branch can be presented by

$$\mathrm{J}(S^*, X^*, E^*) = \begin{bmatrix} -[\frac{1}{\tau^*} + A_4] & -A_2 & A_3 \\ A_4 & 0 & -A_3 \\ A_7 & A_8 & -A_9 \end{bmatrix},$$

The term $J(2,2)$ was evaluated using the following relation

$$\left[\frac{R^* - 1 - b_H^* \tau^*}{\tau^*}\right] = -\frac{S^*}{(1 + S^* + \gamma_1 E^{*2})}.$$

Here the solutions are physically meaningful if $A_i > 0,\ i = 1, ..., 9, i \neq 6, 7$. Thus the characteristic polynomial of $J(S^*, X^*, E^*)$ is given by,

$$\begin{aligned} F(\lambda) &= \lambda^3 + c_1\lambda^2 + c_2\lambda + c_3, \\ c_1 &= \frac{1}{\tau^*} + A_9 + A_1, \\ c_2 &= \frac{A_9}{\tau^*} + A_4 A_2 - A_7 A_3 + A_8 A_3 + A_4 A_9, \\ c_3 &= \frac{A_8 A_3}{\tau^*} - A_2 A_3 A_7 + A_9 A_4 A_2. \end{aligned} \tag{23}$$

Thus, it is sufficient (using the well-known Routh–Hurwitz criteria [24]) to establish that $c_1 > 0$, $c_3 > 0$ and $c_1 c_2 - c_3 > 0$, to confirm that all the roots of $F(\lambda)$ have negative real parts.

Clearly $c_1 > 0$. To prove that $c_3 > 0$, we have

$$c_3 = \frac{A_8 A_3}{\tau^*} - A_2 A_3 A_7 + A_9 A_4 A_2 = \frac{A_8 A_3}{\tau^*} + A_2[A_4 d_1 + A_3 d_2] > 0.$$

$$d_1 = \frac{(\beta_2 - R_2^*)}{\tau^*}, d_2 = \frac{q(p^* S^*)^q [e^{-(p^* S^*)^q}] fl_3\, X^*}{\left(1 + S^* + \gamma_1 e^{*2}\right)}.$$

For positive solutions, we have $A_i > 0,\ i = 1, ..., 9, i \neq 6, 7$, Hence, $c_3 > 0$.

We now examine the expression $c_1 c_2 - c_3$. After some manipulations, we find that

$$\begin{aligned} c_1 c_2 - c_3 &= \left(A_3 A_7 + {A_4}^2\right) A_2 + (A_4 + A_9)(+A_3 A_8 + A_4 A_9 - A_3 A_7) \\ &\quad + \frac{A_4 A_2 - A_7 A_3 + 2 A_4 A_9 + {A_9}^2}{\tau} + \frac{A_9}{\tau^2}, \\ &= \left(A_3 A_7 + {A_4}^2\right) A_2 + (A_4 + A_9)(A_3[A_8 + d_2] + A_4 d_1) \\ &\quad + \frac{A_4\,[d_1 + A_2 + A_9] + A_3 d_2 + {A_9}^2}{\tau} + \frac{A_9}{\tau^2} > 0, \end{aligned}$$

Thus, we conclude, using Routh–Hurwitz criteria, that all the roots of the characteristic polynomial $F(\lambda)$ have negative real parts. Therefore, we have the following result:

Lemma 3. *Whenever the no-washout branch $X^* = (S^*, X^*, E^*)$ is positive, it is locally asymptotically stable.*

6. Numerical Discussion

In this section, we move on to study the time evolution of the model solutions of Equations (9)–(11). The initial value problem was integrated using the Runge–Kutta based ODE45 solver of MATLAB. We start by showing the bioreactor dynamics for the case of $\beta_1 = 1$ and different values of the recycle ratio ($R^* = 0$, 0.5 and 1). This corresponds to a continuous flow with no recycle ($R^* = 0$), with a non-ideal recycle ($R^* = 0.5$) and with an ideal recycle ($R^* = 1$). The rest of the model's dimensionless parameters are shown in Table 2. The simulations are shown in Figure 2 for startup conditions $S = 100$ g/L, $X = 4.32$ g/L and $E = 0$. This corresponds to $(S^* = 1.53, X^* = 1, E^* = 0)$. The figures show a similar trend for all values of R^*. The substrate concentration decreases quickly for a short time, reaches a minimum and then increases to reach a constant value. This is a typical example of an inverse response. This behavior is also shown in the biomass profile as the biomass concentration reaches a maximum and then decreases due to the inhibition effects of ethanol. The profile of ethanol concentration shows, on the other hand, a steady increase until an asymptotic value is reached.

The effect of recycle ratio is shown in the diagram. It can be seen that bioethanol concentration substantially increases as the recycling ratio is increased. In fact the increase in bioethanol concentration is around 43% when the bioreactor is operated with no recycle ($R^* = 0$) compared to $R^* = 0.5$.

The effect of latency of ethanol production is investigated by numerically varying the parameter p^* for the same residence time $\tau = 12$ and start-up conditions as Figure 2 but with an ideal recycle $R^* = 1$, since it yields the highest ethanol concentration. Although p^* is not an operating parameter, it is important to study its effect on the performance of the process. Figure 3 shows the effect of different values of p^* ($p^* = 0$, 0.5, 1 and 10). First, it can be seen that the inverse response, which is the feature of the inhibition effect of ethanol, is also maintained in this figure; however, it is attenuated as the delay is increased. As expected, the ethanol concentration decreases as the delay is pronounced. For example, the decrease in ethanol concentration is around 23.8% when the delay is increased from $p^* = 0$ to $p^* = 1$.

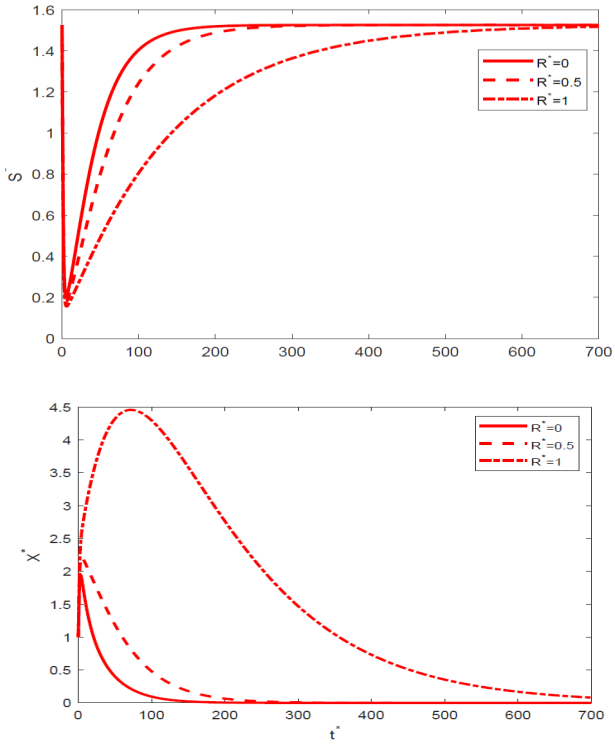

Figure 2. *Cont.*

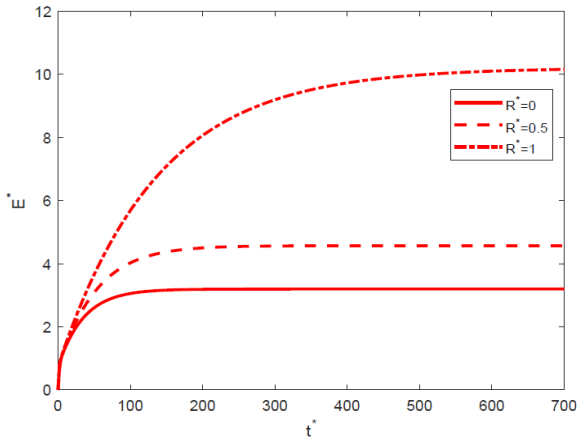

Figure 2. Time evolutions by varying recycle ratio R^* with a fixed initial profile ($S^* = 1.53, X^* = 1, E^* = 0$) and the rest of parameters of Table 2.

The effect of varying the bioreactor residence time τ^* is shown in Figure 4. τ^* was varied from 1, 6, 12, to 20. A large ethanol concentration is obtained for small residence times (i.e., larger dilution rates). The increase in the residence time rate almost linearly affects the decrease in ethanol concentration. An increase in residence time from $\tau^* = 1$ to $\tau^* = 6$ decreases the asymptotic value of ethanol concentration by 10.5%.

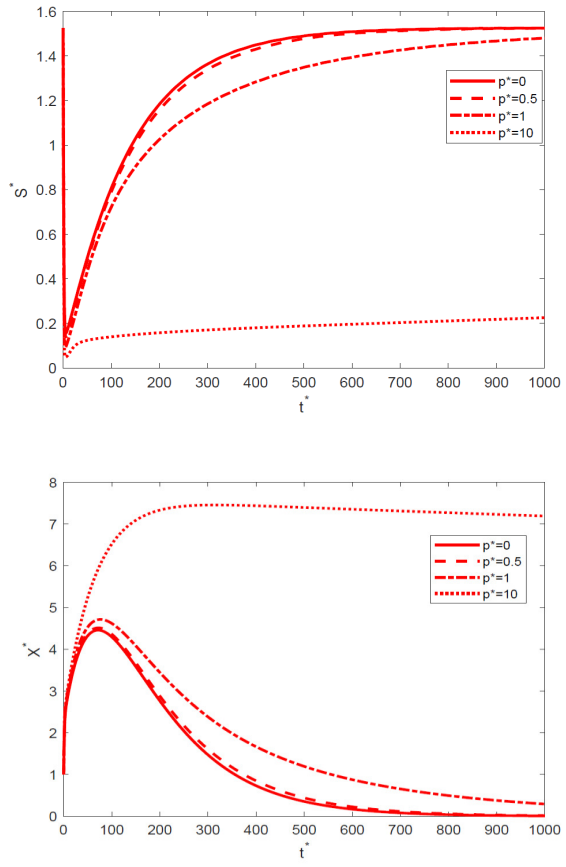

Figure 3. *Cont.*

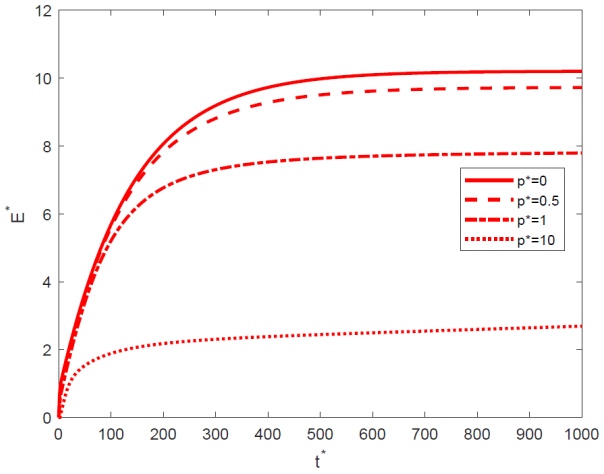

Figure 3. Time evolutions by varying p^* with a fixed initial profile $(S^* = 1.53, X^* = 1, E^* = 0)$, $R^* = 1$ and the rest of parameters of Table 2.

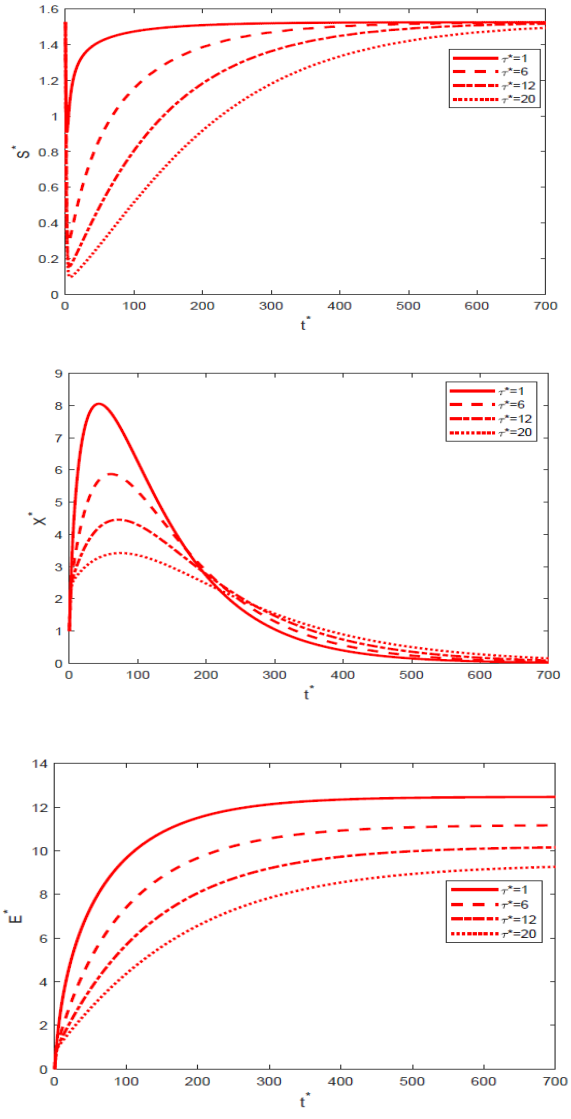

Figure 4. Time evolutions by varying residence time τ^* with a fixed initial profile $(S^* = 1.53, X^* = 1, E^* = 0)$, $R^* = 1$ and the other parameters of Table 2.

Finally, we examine the effect of the purge fraction β_1. In order to avoid a washout solution, as predicted by Equation (22) for $R^* = \beta_1$, and to allow for the study of variations of β_1, the effective recycle ratio R^* was fixed at 0.5 and β_1 was allowed to vary from 0.5, 0.75 to 1. It can be seen from Figure 5 that the highest ethanol concentration occurs at the smallest values of the purge fraction. However, a careful choice of values of β_1 and R^* should be made to avoid washout conditions.

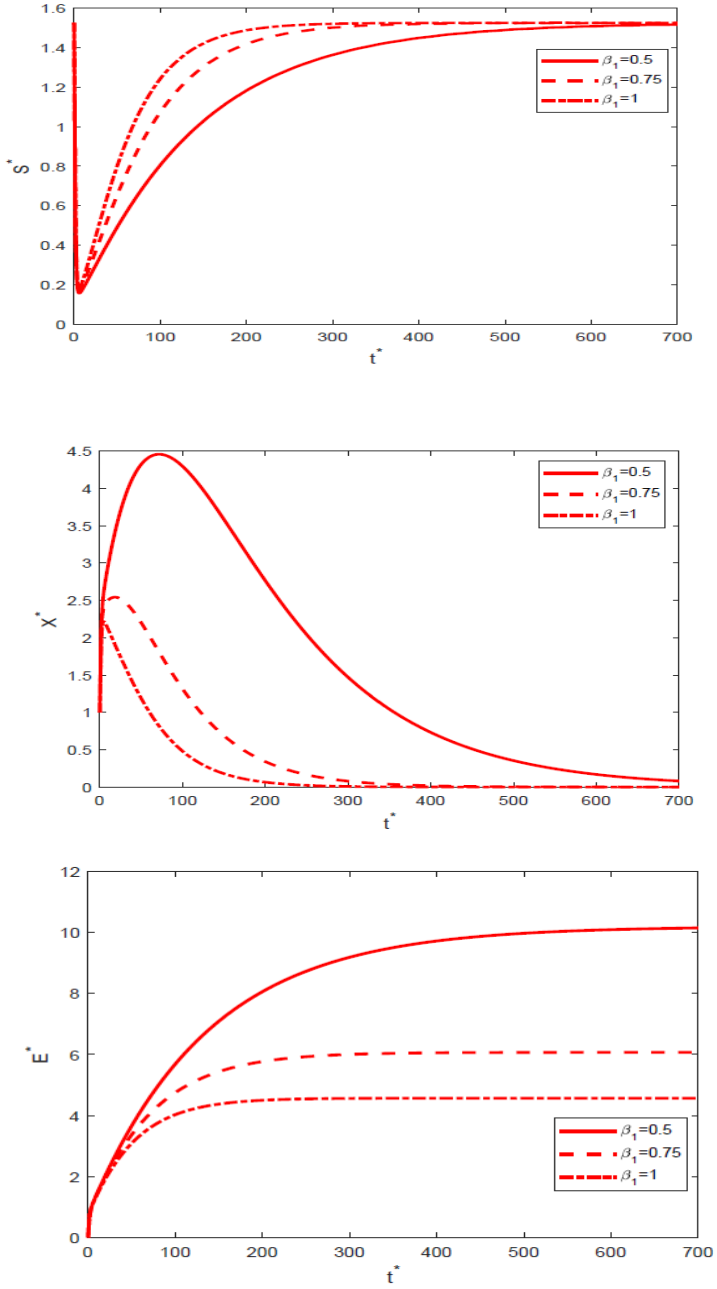

Figure 5. Time evolutions by varying purge fraction β_1 with a fixed initial profile ($S^* = 1.53, X^* = 1, E^* = 0$), $R^* = 0.5$ and the rest of parameters of Table 2.

7. Conclusions

In this study, a mathematical reactor model with Andrew's growth rate and latency of ethanol production was developed to study the dynamical behaviour of continuous fermentation in reactor with recycle using parameter values from batch experimental data [3–18]. The positivity and the boundedness of model solutions were confirmed under reasonable restrictions on parameters. The stability analysis of the steady state solutions yielded an analytical expression for the critical residence time at which a stability exchange between washout and non-trivial solution occurs. We observed that this critical value of residence time is dependent on the feed substrate concentration, purge fraction and the recycle ratio. Therefore, a careful choice of these operating parameters can avoid washout conditions. Numerical simulations provided useful qualitative trends of the dynamics of the process. An inverse response was observed in the profile of substrate and biomass concentrations. This dynamic behavior has practical implications when feedback control is desired to maintain the process at certain set points [12], since such systems are more difficult to control. It was found that the maximum ethanol concentration is obtained at the maximum allowable recycle ratio, the smallest purge fraction and largest dilution rate. However, care should be taken to optimize the selection of such parameters to avoid washout conditions. A final note should be made about the proposed model's strengths and limitations. Since the model kinetics were extracted from a validated batch experiment, and since the operating parameters were numerically varied around realistic values, this provided the obtained results with a fair degree of credibility. However, the proposed model could be improved by taking some important parameters that affect the fermentation process into consideration, such as medium temperature and acidity. The analysis carried out in the paper was limited to steady state behavior, but could be used in the future to address the complex phenomena associated with the occurrence of oscillatory behavior in continuous ethanol fermentation as result of dynamic bifurcations [11].

Author Contributions: R.T.A.: Formal analysis, Methodology, Writing—original draft, Writing—review editing; S.K.B.: Formal analysis, Software, Writing—original draft, Writing—review editing; A.A.: Software, Writing—original draft, Writing—review editing; M.B.: Software, Writing—review editing. All authors have read and agreed to the published version of the manuscript.

Funding: The authors extend their appreciation to the Deanship of Scientific Research at King Saud University for funding this work through research group No. (RG-1441-188).

Institutional Review Board Statement: Not applicable.

Informed Consent Statement: Not applicable.

Conflicts of Interest: The authors declare no conflict of interest.

Nomenclature

Symbol	Units	Description
F	$\mathrm{L\,h^{-1}}$	Flow rate through the reactor
b_H	$\mathrm{h^{-1}}$	Death coefficient
b_H^*		Dimensionless death rate $[b_H^* = b_H/\mu_{\max}]$
K_s	$\mathrm{g_s L^{-1}}$	Saturation constant
S	$\mathrm{g\ L^{-1}}$	Substrate concentration within the reactor
S^*	-	Dimensionless substrate concentration within the reactor $[S^* = S/K_s]$
S_0	$\mathrm{g\ L^{-1}}$	Concentration of substrate flowing into the reactor
S_0^*	-	Dimensionless substrate concentration in the feed $[S_0^* = S_0/K_s]$
V	L	Volume of the reactor
X	$\mathrm{g\ L^{-1}}$	Biomass concentration within the reactor
X^*	-	Dimensionless biomass concentration within the reactor $[X^* = X/Y_{x/s}K_s]$
E	$\mathrm{g\ L^{-1}}$	Ethanol concentration within the reactor
E^*	-	Dimensionless ethanol concentration within the reactor $[E^* = E/K_s]$

Symbol	Units	Description
t	h	Time
t^*	-	Dimensionless time [$t^* = \mu_{\max} t$]
$Y_{x/s}$	$g_b g_s^{-1}$	Biomass yield coefficient
$Y_{e/x}$	$g_e g_b^{-1}$	Ethanol/biomass yield coefficient
γ	$g_e g_b^{-1} h^{-1}$	Kinetic constant of ethanol production by maintenance
K_e	$L\, g_s (g_e^2)^{-1}$	Inhibition constant by ethanol
γ_1	-	Dimensionless inhibition constant by ethanol [$\gamma_1 = K_e K_s$]
$M_2(S,e)$	h^{-1}	Specific growth rate model
$\mu_{\max}$	h^{-1}	Maximum specific growth rate
τ	h	Residence time
τ^*	-	Dimensionless residence time [$\tau^* = V\mu_{\max}/F$]
R_i	-	Recycle ratio based on volumetric flow rates
R_i^*	-	Effective recycle parameter [$R_i^* = (\mathcal{C}-1)R_i$]
γ_2	-	[$\gamma_2 = \gamma Y_{x/s}$]
γ_3	-	[$\gamma_3 = Y_{x/s}\, Y_{e/x}$]
p^*	-	[$p^* = pK_s$]

References

1. Martins, F.; Felgueiras, C.; Smitkova, M.; Caetano, N. Analysis of fossil fuel energy consumption and environmental impacts in European countries. *Energies* **2019**, *12*, 964. [CrossRef]
2. Comelli, R.N.; Isla, M.A.; Seluy, L.G. Wastewater from the soft drinks industry as a source for bioethanol production. *Bioresour. Technol.* **2013**, *136*, 140–147.
3. Comelli, R.N.; Seluy, L.G.; Isla, M.A. Performance of several saccharomyces strains for the alcoholic fermentation of sugar-sweetened high-strength wastewaters: Comparative analysis and kinetic modelling. *J. Biotechnol.* **2016**, *33*, 874–882. [CrossRef]
4. Huynh, L.H.; Ismadji, S.; Ahmed, I.N.; Nguyen, P.L.T.; Hsu, J.Y. Bioethanol production from pretreated melaleuca leucadendron shedding bark simultaneous saccharification and fermentation at high solid loading. *Bioresour. Technol.* **2013**, *136*, 213–221.
5. Bhowmik, S.K.; Alqahtani, R. Mathematical analysis of bioethanol production through continuous reactor with a settling unit. *Comput. Chem. Eng.* **2018**, *111*, 241–251. [CrossRef]
6. Nikolaos, C.K.; Nikolaos, N.; Nikolas, P.; Konstantinos, M.; Sophia, M.; Athanassios, C.M. Two-step conversion of LLCN olefins to strong anti-knocking alcohol mixtures catalysed by Rh, Ru/TPPTS complexes in aqueous media. *Catal. Today* **2015**, *247*, 132–138.
7. Palmarola-Adrados, B.; Choteborska, P.; Galbe, M.; Zacchi, G. Ethanol production from non-starch carbohydrates of wheat bran. *Bioresour. Technol.* **2005**, *96*, 843–850. [CrossRef] [PubMed]
8. Kaparaju, P.; Serrano, M.; Thomsen, A.B.; Kongjan, P.; Angelidaki, I. Bioethanol, biohydrogen and biogas production from wheat straw in a biorefinery concept. *Bioresour. Technol.* **2009**, *100*, 2562–2568. [CrossRef]
9. Aimaretti, N.R.; Ybalo, C.V.; Rojas, M.L.; Plou, F.J.; Yori, J.C. Production of bioethanol from carrot discards. *Bioresour. Technol.* **2012**, *123*, 727–732. [CrossRef]
10. Njoku, S.A.; Xahring, B.K.; Uellendahl, H. Pretreatment as the crucial step for a cellulosic ethanol biorefinery: Testing the efficiency of wet explosion on different types of biomass. *Bioresour. Technol.* **2012**, *124*, 105–110. [CrossRef]
11. Ciesielski, A.; Grzywacz, R. Dynamic bifurcations in continuous process of bioethanol production under aerobic conditions using *Saccharomyces cerevisiae*. *Biochem. Eng. J.* **2020**, *161*, 107609. [CrossRef]
12. Ajbar, A.; Ali, E. Study of advanced control of ethanol production through continuous fermentation. *J. King Saud Univ. Eng. Sci.* **2017**, *29*, 1–11. [CrossRef]
13. Wei, P.; Cheng, L.; Zhang, L.; Xu, X.; Chen, H.; Gao, C. A review of membrane technology for bioethanol production. *Renew. Sustain. Energy Rev.* **2014**, *30*, 388–400. [CrossRef]
14. Astudillo, I.C.P.; Alzate, C.A.C. Importance of stability study of continuous systems for ethanol production. *J. Biotechnol.* **2011**, *151*, 43–55. [CrossRef] [PubMed]
15. Sridhar, L.M. Elimination of oscillations in fermentation processes. *AIChE J.* **2011**, *57*, 2397–2405. [CrossRef]
16. Mahecha-Botero, M.; Garhyan, P.; Elnashaie, S.S.E.H. Bifurcation, stabilization, and ethanol productivity enhancement for a membrane fermentor. *Math. Comput. Model.* **2005**, *41*, 391–406. [CrossRef]
17. Andrews, J.F. A mathematical model for the continuous culture of microorganisms utilizing inhibitory substrates. *Biotechnol. Bioeng.* **1968**, *10*, 707–723. [CrossRef]
18. Yoon, S.H.; Lee, S. Critical operational parameters for zero sludge production in biological wastewater treatment processes combined with sludge disintegration. *Water Res.* **2005**, *39*, 3738–3754. [CrossRef]
19. Rao, M.R.M. *Ordinary Differential Equations, Theory and Applications*; Affiliated East-West Press: Delhi, India, 1980.
20. Coddington, E.A.; Levinson, N. *Theory of Ordinary Differential Equations*; McGraw-Hill: New York, NY, USA, 1955.
21. Gouze, J.L.; Serhani, M.; Raissi, N. Dynamical study and robustness for a nonlinear wastewater treatment model. *Nonlinear Anal. Real. World Appl.* **2011**, *12*, 487–500.

22. Boutanfit, H.; Serhani, M.; Boutoulout, A. Sensitivity and strong controllability of a nonlinear chemostat model. *ESAIM Proc. Surv.* **2015**, *49*, 115–129.
23. Quigley, J.L.; Nelson, M.I.; Chen, X.D. A fundamental analysis of continuous flow bioreactor and membrane reactor models with non-competitive product inhibition. *Asia-Pac. J. Chem. Eng.* **2009**, *4*, 107–117.
24. May, R.M. *Stability and Complexity in Model Ecosystems*; Princeton University Press: Princeton, NJ, USA, 1973.